

Formic Acid Decomposition on the {110}-Microfaceted Surface of TiO₂(100): Insights Derived from ¹⁸O-Labeling Studies

Michael A. Henderson

Materials and Interfaces Group, Environmental Molecular Sciences Laboratory, Pacific Northwest Laboratory,[†] PO Box 999, MS K2-12, Richland, Washington 99352

Received: June 5, 1995; In Final Form: August 9, 1995[⊗]

The decomposition of formic acid was examined on the {110}-microfaceted surface of TiO₂(100) with temperature-programmed desorption (TPD), static secondary ion mass spectrometry (SSIMS), low-energy electron diffraction (LEED), and work function measurements. No ordered structures of formic acid, or of its main decomposition product formate, were observed. Formic acid decomposed on TiO₂(100) to formate and a surface proton at temperatures below 250 K. The main TPD products were water, which desorbed below 450 K, and CO, which desorbed at 555 K. Formaldehyde was also observed as a TPD product at 540 K. CO and formaldehyde resulted from formate decomposition. TPD experiments performed on the ¹⁸O-enriched surface show that extensive isotopic oxygen incorporation occurred for the CO, water, and formaldehyde TPD products. The incorporation of lattice ¹⁸O into the water product indicates that the acid proton, deposited during formic acid decomposition, was able to abstract oxygen from the surface. SSIMS measurements indicate that incorporation of lattice ¹⁸O into the formate species did not occur until the onset of formate decomposition, implying that lattice oxygen atoms were involved in the formate decomposition process. Studies with coadsorbed H₂¹⁸O indicate that water was a mild site blocker of formic acid adsorption and/or decomposition sites and that little or no isotopic oxygen exchange took place between the two adsorbed molecules.

1. Introduction

The decomposition of formic acid has been studied on rutile TiO₂(110)^{1–4} and TiO₂(001),^{5–7} as well as on single-crystal surfaces of other oxides.^{8–13} Formic acid decomposes almost exclusively to formate species on titanium dioxide single crystal surfaces. Formate, in turn, decomposes above 450 K by either dehydration to CO and H₂O or dehydrogenation to CO₂ and H₂. The dehydration mechanism is believed to occur by way of unimolecular decomposition of formate,^{3,6} while the dehydrogenation process may involve unimolecular or bimolecular processes.

Formic acid chemistry has not been examined on the (100) surface of TiO₂. The (100) surface possesses two stable structures under ultrahigh-vacuum (UHV) conditions: the bulk-terminated structure and the {110}-microfaceted structure. The {110} microfaceting of TiO₂(100) results in a well-ordered (1 × 3) surface structure,^{14–23} schematically shown in Figure 1. The (1 × 3) surface possesses three unique Ti cation sites, with an approximate total surface density of 7.4 × 10¹⁴ cm⁻², as well as two-coordinate bridging O anion sites. The (1 × 3) surface is slightly reduced based on photoemission studies.^{14–17,19,21} The reduced centers are believed to be three-coordinate Ti³⁺ atoms located at the ridges of each facet, comprising one-third of the surface Ti cation sites.¹⁹ The influence of low coordination and/or reduced Ti cations sites on the chemistry of formic acid has been addressed by Barteau et al.^{5,6,24} In general, these sites are linked to the production of formaldehyde. Barteau et al. have identified two mechanisms by which formaldehyde is produced from formic acid decomposition on ion sputtered and annealed TiO₂(001). One mechanism involves a bimolecular reaction between two formate

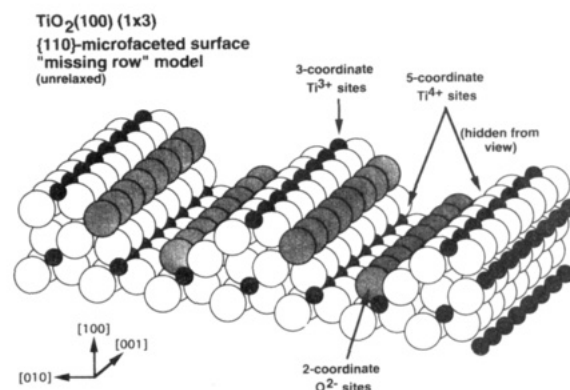


Figure 1. Schematic model of the {110}-microfaceted surface of TiO₂(100). The facets form a (1 × 3) structure.

species adsorbed on the same four-coordination surface Ti⁴⁺ site. The other mechanism involves reduction of formate by lower valency cation sites. The production of formaldehyde from formic acid decomposition has also been observed by Gercher and Cox on defective SnO₂(110)¹⁰ and by Dilara and Vohs at low coordination Zr⁴⁺ sites on ZrO₂(100).¹²

The extent to which lattice oxygen atoms are involved in formic acid chemistry has not been experimentally addressed in previous studies. In this study, formic acid decomposition was examined on the {110}-microfaceted surface of TiO₂(100) with emphasis on the role that lattice oxygen atoms play in the formate decomposition process. This was accomplished by enriching the TiO₂(100) surface with ¹⁸O. TPD and SSIMS measurements were used to characterize the incorporation of ¹⁸O into surface species and gaseous products during formic acid and formate decomposition.

2. Experimental Section

The ultrahigh-vacuum chamber and methods used in this study are discussed in more detail elsewhere.²² Mounting and

[†] Pacific Northwest Laboratory is a multiprogram national laboratory operated for the U.S. Department of Energy by Battelle Memorial Institute under Contract DE-AC06-76RLO 1830.

[⊗] Abstract published in *Advance ACS Abstracts*, September 15, 1995.

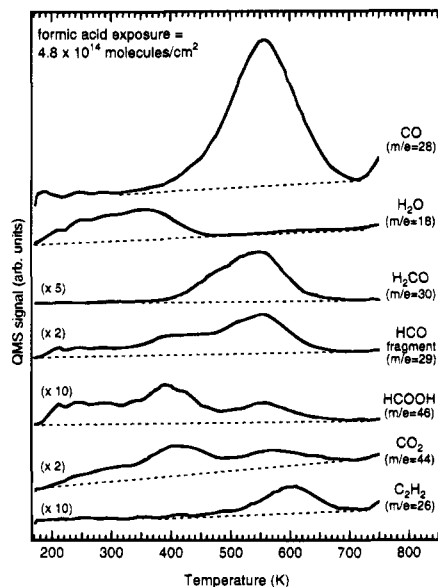


Figure 2. TPD spectra from a formic acid exposure of 4.8×10^{14} molecules/cm² (monolayer saturation) to the TiO₂(100) (1 × 3) surface at 170 K. Spectra are displaced vertically for clarity, and base lines are shown to highlight important TPD features.

cleaning of the TiO₂(100) crystal are also discussed in this previous work. The {110}-microfaceted surface of TiO₂(100), hereafter referred to as the (1 × 3) surface, was prepared by annealing the fully oxidized surface at 840 K in UHV. The LEED pattern from this surface shows third-order spots along the [010] direction.²² The fully oxidized surface, which is designated as the (1 × 1) surface based on LEED,²² was prepared by oxidizing the 500 eV Ar⁺ ion-sputtered surface in 1×10^{-6} Torr of oxygen at 750 K. The ¹⁸O-enriched surface was prepared by oxidizing with ¹⁸O₂ prior to forming the (1 × 3) surface. SSIMS indicated that the ¹⁸O to ¹⁶O ratio for ¹⁸O-enriched (1 × 3) surface prepared in this manner was about 2.5 to 1. The ramp rate for all TPD and temperature-programmed SSIMS experiments was 2 K/s. Some TPD traces were Fourier filtered to enhance the appearance of the data. SSIMS measurements were performed with a differentially pumped ion gun and a quadrupole-based spectrometer (Extrel C50). The primary ion flux was maintained in the nA/cm² regime to minimize surface damage while obtaining satisfactory signal-to-noise in the data. The designations “+SSIMS” and “-SSIMS” used throughout the paper refer to the selective detection of positive and negative secondary ions, respectively.

Formic acid was dosed on the TiO₂(100) surface through a translatable directional doser. Accurate and reproducible gas exposures were obtained by means of a micron-sized pinhole. Formic acid (HCOOH, A.C.S. reagent grade, 96% purity) was obtained from Aldrich. The major impurities, according to the supplier, were acetic acid (<0.4%) and water. Freeze-pump-thaw cycles with liquid nitrogen were performed on the formic acid before use. Additionally, the gas handling system and doser assembly were conditioned to new exposures of formic acid at the beginning of each day.

3. Results and Discussion

3.1. TPD Results from the Clean (1 × 3) Surface. No ordered LEED patterns were observed for formic acid on the (1 × 3) surface of TiO₂(100), although a (1 × 2) surface structure has been observed from formate on TiO₂(110).^{1,3,4}

Figure 2 shows TPD spectra of the products from decomposition of a 4.8×10^{14} molecules/cm² exposure of formic acid on the TiO₂(100) (1 × 3) surface. The dominant products were

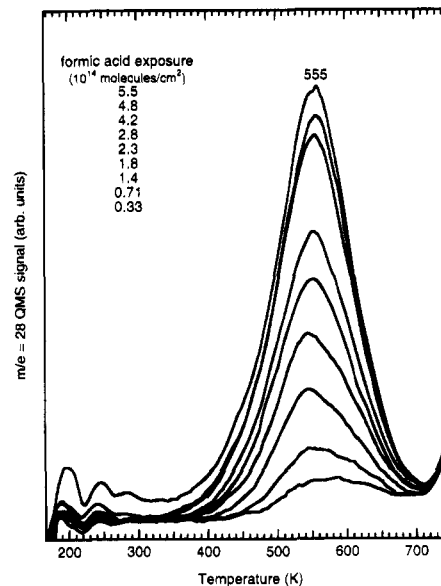


Figure 3. TPD spectra of CO ($m/e = 28$) as a function of formic acid exposure to the TiO₂(100) (1 × 3) surface at 170 K.

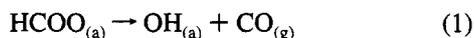
water, which desorbed below 450 K, and CO, which desorbed in a broad peak centered at about 555 K. Significant desorptions of the parent molecule and of formaldehyde were also detected near 555 K. The majority of the QMS intensity at $m/e = 44$ resulted from the CO₂⁺ cracking fragment of the parent HCOOH molecule, as seen by comparison with the $m/e = 46$ trace. However, the $m/e = 44$ and 46 signals did not perfectly track each other in relative intensity over the entire temperature range, implying that some of the $m/e = 44$ signal may result from a small amount of CO₂ desorption. Desorption of molecular hydrogen or oxygen was not observed. Desorption of small amounts of acetylene and ketene (the latter is not shown) were detected at 600 and 570 K, respectively. Acetylene was not observed from formic acid decomposition on the (1 × 1) surface of TiO₂(100) (see below), on TiO₂(001),^{5,6,24} or on TiO₂(110),³ but acetylene was observed on ZrO₂(100).¹⁰ Ketene is a major decomposition product of acetic acid on TiO₂(001)⁵ and in this study was the result of an acetic acid impurity in the formic acid (see Experimental Section) based on TPD results from adsorbed acetic acid on TiO₂(100) (not shown). TPD data for the QMS cracking fragment HCO⁺ ($m/e = 29$), included in Figure 2, have contributions from both H₂CO and HCOOH desorption. This fragment will be used in monitoring the relative degree of ¹⁸O exchange between the surface and these two TPD products (see below).

Figure 3 shows CO TPD spectra resulting from various exposures of formic acid on the TiO₂(100) (1 × 3) surface. The desorption of CO from formic acid decomposition was reaction-limited and appeared first order with a peak desorption temperature similar to that observed from TiO₂(001)^{5,6,24} and from TiO₂(110).³ The CO desorption peak was above 560 K after low formic acid exposures, shifted below 550 K for intermediate exposures, and was at about 550 K after formic acid saturation. A small portion of the $m/e = 28$ intensity resulted from QMS cracking of H₂CO, but this contribution to the TPD data of Figure 3 should be negligible. (The small “peaks” below 300 K were the result of oscillations at the start of the temperature ramp and correspond to desorption of background CO adsorbed on the heating leads.)

The TPD spectra for water desorption as a function of formic acid exposure are shown in Figure 4. Decomposition of low formic acid exposures resulted in at least two H₂O TPD states between 300 and 500 K. The lower temperature state at 325 K

resembles that observed from TPD of low coverages of water on the clean TiO₂(100) (1 × 3) surface,²² but the higher temperature state at 430 K does not have an analog from water on the clean surface. As the formic acid exposure was increased, the peaks seen at low exposure melted into a single desorption feature centered at 355 K. The high-temperature tail above 450 K was no longer present at high formic acid exposures. (The features below 270 K were caused by oscillations at the start of the temperature ramp.) At high HCOOH exposures a broad, weak water state was present at 630 K. The absence of an intense water desorption peak at 555 K to match the desorption of CO does not have an obvious explanation. Dehydration of formate should produce 1 equiv of water per every 2 equiv of CO. However, based on TPD, the formate hydrogen atom does not produce water when formate decomposes. Some of the hydrogen ends up in the formaldehyde, formic acid, and acetylene products (see Figure 2), but since these are minority species, it appears that most of the formate hydrogen does not evolve from the surface in TPD. It may be that the undetected hydrogen diffuses into the bulk of the oxide.

Figure 5 shows TPD spectra from formic acid (*m/e* = 46) as a function of formic acid exposure on the TiO₂(100) (1 × 3) surface. Little or no formic acid desorption occurred for formic acid exposures below 1.0 × 10¹⁴ molecules/cm², indicating complete decomposition. Two formic acid desorption features appeared simultaneously in TPD for exposures above 1.0 × 10¹⁴ molecules/cm² and increased in intensity with increasing exposure. The lower temperature formic acid desorption state shifted from 450 to 390 K with increasing exposure. The high-temperature formic acid desorption feature (at 555 K) showed little or no coverage dependence but mirrored the shape and peak temperature of the CO TPD feature (Figure 3). The coincidence of the 555 K formic acid peak with the evolution of CO in TPD suggests that formate decomposition feeds the surface with protons, forming hydroxyl groups which are available for reaction with other formate species to produce formic acid. The 555 K formic acid desorption state is therefore assigned to the recombination of formate and a proton/hydroxyl group, according to eqs 1–3.



(The fate of the O_(a) in eq 2 is unknown since no O₂ desorption was detected, and little or no CO₂ was detected.) It is also possible that formic acid desorption results from a bimolecular process based on the coverage dependency in TPD. The availability of surface protons may have a significant influence on whether formate is protonated and desorbs as formic acid or whether formate decomposes or reacts to form other C₁ species.

The 390–450 K temperature formic acid TPD feature somewhat parallels the water TPD peak, particularly at low formic acid exposures. Based on photoemission assignments of formate, similar formic acid TPD states observed from TiO₂(001)^{5,6,24} and from TiO₂(110)^{1,3} have been assigned to recombinative desorption of formic acid. Also, a similar formic acid TPD state was assigned to recombinative desorption from thin film NiO(100) based on HREELS measurements.⁹

Low-temperature (<300 K) desorption states of formic acid appeared in TPD for formic acid exposures above 4.0 × 10¹⁴ molecules/cm². These states are tentatively assigned to weakly bound formic acid molecules in the monolayer and/or second

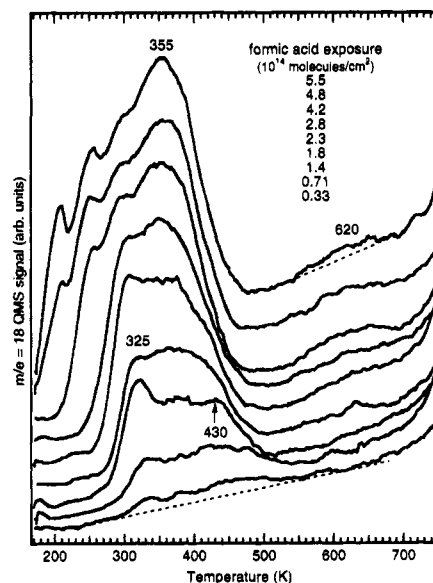


Figure 4. TPD spectra of H₂O (*m/e* = 18) as a function of formic acid exposure to the TiO₂(100) (1 × 3) surface at 170 K. Spectra are displaced vertically for clarity.

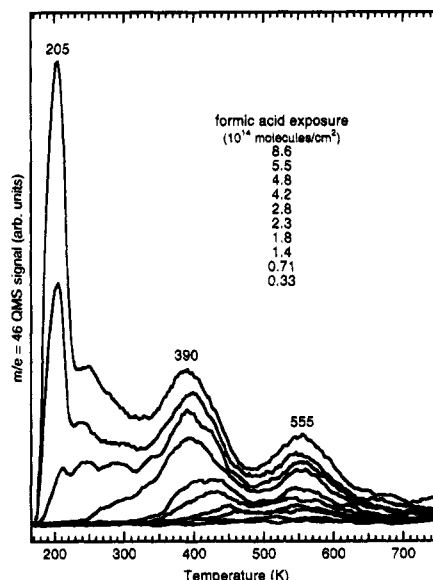


Figure 5. TPD spectra of HCOOH (*m/e* = 46) as a function of formic acid exposure to the TiO₂(100) (1 × 3) surface at 170 K.

layer. The sharp desorption feature at 205 K was largely the result of the thermal “spike” which occurred during initiation of the temperature ramp. Although this feature cannot be strictly interpreted, the formic acid molecules which desorbed below 220 K originated from the TiO₂(100) surface. The 205 K desorption intensity did not increase with formic acid exposures above about 9 × 10¹⁴ molecules/cm², implying it resulted from second layer formic acid. (Multilayer formic acid is not stable at 170 K under UHV conditions¹³ so adsorption at 170 K should stop at the first or second layers.)

Figure 6 shows TPD spectra for H₂CO (*m/e* = 30) as a function of formic acid exposure. Formaldehyde was observed over the entire formic acid exposure range, but the yield was not linear with formic acid exposure until the exposure exceeded about 1.0 × 10¹⁴ molecules/cm². The formaldehyde TPD peak showed a slight coverage dependence as a function of formic acid exposure and maximized at 540 K. This temperature places formaldehyde desorption on the lower temperature side of the CO and formic acid TPD states.

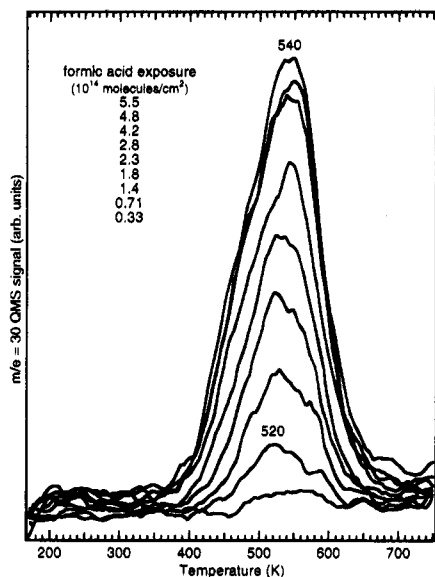


Figure 6. TPD spectra of H_2CO ($m/e = 30$) as a function of formic acid exposure to the $\text{TiO}_2(100)$ (1×3) surface at 170 K.

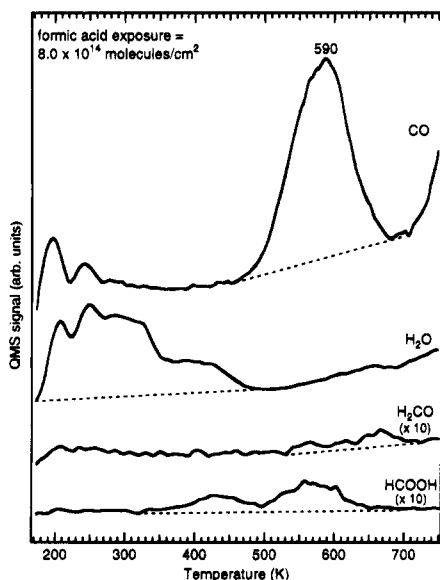


Figure 7. TPD spectra from a formic acid exposure of 8.0×10^{14} molecules/ cm^2 on the $\text{TiO}_2(100)$ (1×1) surface at 170 K. Spectra are displaced vertically for clarity.

As a point of comparison for the (1×3) surface, the TPD spectra resulting from decomposition of a 8.0×10^{14} molecules/ cm^2 formic acid exposure on the (1×1) surface is shown in Figure 7. The major difference between the TPD products from HCOOH decomposition on the (1×1) and (1×3) surfaces is that formaldehyde was not a product from the (1×1) surface. This result is not surprising since formaldehyde production has been linked to the presence of low coordination and/or reduced surface cation sites.^{5,6,24} The (1×1) surface is fully oxidized and possesses Ti cation sites which are five-coordinate and $4+$. The small amount of formaldehyde that was desorbed in Figure 7 occurred above the onset temperature at which the micro-faceting process begins.²² Acetylene was also not observed from the (1×1) surface and therefore is linked to the presence of Ti^{3+} sites. Subtle differences exist in the CO, HCOOH , and H_2O desorption peak profiles from the two surfaces. The CO desorption peak from the (1×1) surface was more narrow and peaked about 30 K higher than for the (1×3) surface. For water, a greater amount of desorption occurred between 350 and 500 K from the (1×1) surface compared to the (1×3)

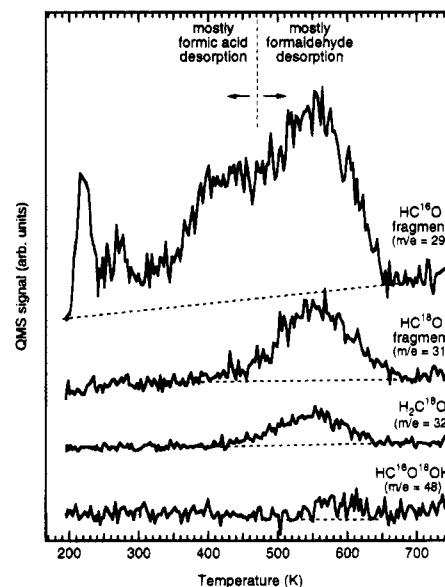


Figure 8. TPD spectra for the HC^{16}O^+ ($m/e = 29$) and HC^{18}O^+ ($m/e = 31$) QMS cracking fragments and for $\text{H}_2\text{C}^{18}\text{O}$ ($m/e = 32$) and $\text{HC}^{16}\text{O}^{18}\text{OH}$ ($m/e = 48$) from a 6.0×10^{14} molecules/ cm^2 formic acid exposure on the ^{18}O -enriched $\text{TiO}_2(100)$ (1×3) surface at 190 K.

surface. Much less HCOOH desorption was observed from the (1×1) surface. Despite these differences between the (1×1) and (1×3) surfaces, there were some similarities. First, little or no CO_2 or H_2 production was observed from either surface. This implies that the dehydrogenation of formate does not readily occur on either surface. Formate dehydrogenation was observed on $\text{TiO}_2(001)$ ^{5,6,24} and $\text{TiO}_2(110)$.^{2,3} Second, only trace amounts of water were observed coincident with CO desorption, with the vast majority of water desorbing below 450 K. Third, the two recombinative desorption sites of formic acid (at 430 K and coincident with CO evolution) were present from both surfaces.

3.2. TPD and SSIMS Results from the ^{18}O -Enriched (1×3) Surface. TPD results from the decomposition of [^{16}O]formic acid on the ^{18}O -enriched $\text{TiO}_2(100)$ (1×3) surface are shown in Figures 8–10. Data in these figures result from a single TPD experiment corresponding to a formic acid exposure of 6.0×10^{14} molecules/ cm^2 on the ^{18}O -enriched surface.

Figure 8 shows TPD traces from the HC^{16}O^+ QMS cracking fragment ($m/e = 29$), the HC^{18}O^+ QMS cracking fragment ($m/e = 31$), $\text{H}_2\text{C}^{18}\text{O}$ ($m/e = 32$), and $\text{HC}^{16}\text{O}^{18}\text{OH}$ ($m/e = 48$) resulting from [^{16}O]formic acid decomposition on the ^{18}O -enriched $\text{TiO}_2(100)$ (1×3) surface. As mentioned previously, molecular formaldehyde and formic acid desorption both contribute to intensity in the HCO^+ QMS cracking fragment. The dominant contribution to the HCO^+ signal above 470 K came from formaldehyde, and the dominant contribution below 470 K came from formic acid (Figure 2). Figure 8 indicates that incorporation of lattice ^{18}O into the HCO^+ signal occurred almost exclusively in the signal above 470 K, ascribed to formaldehyde desorption. This can be seen by comparing the $\text{H}_2\text{C}^{18}\text{O}$ TPD trace with that of the trace for the HC^{18}O^+ cracking fragment. However, some ^{18}O was also incorporated into the high-temperature formic acid desorption state since a weak desorption signal corresponding to $\text{HC}^{16}\text{O}^{18}\text{OH}$ ($m/e = 48$) occurred at 550–630 K. The reason for the shift in the ^{18}O -containing formic acid desorption temperature relative to the 555 K TPD state on the pure ^{16}O -surface (Figure 5) is unknown. However, since no $\text{HC}^{16}\text{O}^{18}\text{OH}$ signal was detected in the formic acid TPD states below the onset of formate decomposition, lattice oxygen atoms only scramble with oxygen

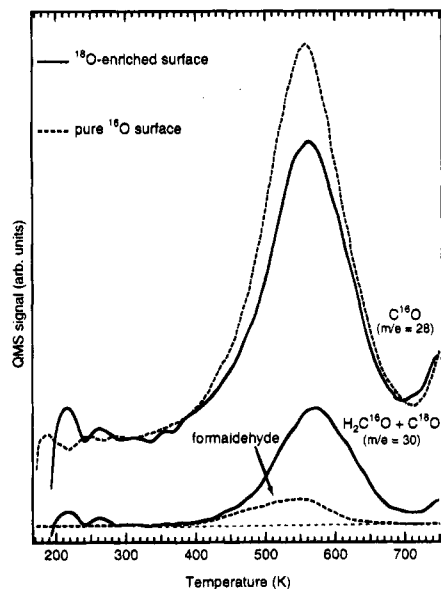


Figure 9. TPD spectra for C¹⁶O ($m/e = 28$) and C¹⁸O ($m/e = 30$) from a 6.0×10^{14} molecules/cm² formic acid exposure on the ¹⁸O-enriched TiO₂(100) (1 × 3) surface at 190 K. The contributions to the $m/e = 28$ signal from C¹⁶O and to the $m/e = 30$ signal from formaldehyde (H₂C¹⁶O) obtained from the pure ¹⁶O-surface are shown for comparison.

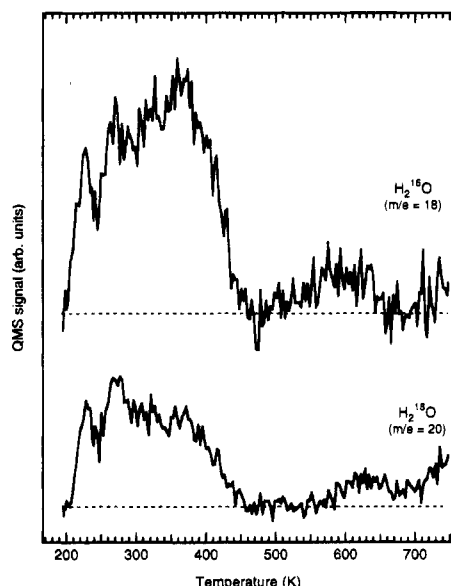


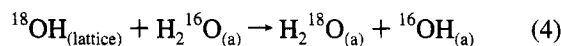
Figure 10. TPD spectra for H₂¹⁶O ($m/e = 18$) and H₂¹⁸O ($m/e = 20$) from a 6.0×10^{14} molecules/cm² formic acid exposure on the ¹⁸O-enriched TiO₂(100) (1 × 3) surface at 190 K. Spectra were displaced vertically, and linear backgrounds were subtracted for clarity.

in adsorbed formate during formate decomposition. This strongly implies that lattice oxygen atoms are involved in the decomposition of formate and/or the formation of formaldehyde.

Figure 9 shows the result from lattice ¹⁸O incorporation into the CO desorption product from [¹⁶O]formic acid decomposition. The C¹⁶O ($m/e = 28$) and H₂C¹⁶O ($m/e = 30$) signals from HCOOH decomposition on the pure ¹⁶O-surface are shown for comparison with the same m/e signals for C¹⁶O and C¹⁸O from the ¹⁸O-enriched surface. As was the case for formaldehyde, Figure 9 indicates that considerable ¹⁸O incorporation occurred for the CO product. This ¹⁸O incorporation resulted in a decreased C¹⁶O signal relative to that for the pure ¹⁶O surface and an increased C¹⁸O desorption signal. The C¹⁸O signal peaked at about 10 K higher temperature than that of the C¹⁶O signal, as was also observed for the high-temperature formic

acid TPD state in Figure 8. This shift should be even greater after deconvolution of whatever formaldehyde signal was present at $m/e = 30$ (as opposed to $m/e = 32$ for the ¹⁸O-containing molecule) in Figure 8. Two possible explanations for the shift are a kinetic isotope effect (¹⁶O versus ¹⁸O) and a surface site effect. The latter would stem from the fact that low coverages of formate yielded CO at slightly higher temperature than observed for higher coverages of formate (Figure 3). Note that oscillations were also present in the C¹⁸O signal below 300 K. This was not due to scrambling of C¹⁶O in the mass spectrometer. A significant background pressure of C¹⁸O was present in the chamber after oxidation of TiO₂(100) with ¹⁸O₂. The oscillations in the $m/e = 28$ and 30 signals result from background C¹⁶O and C¹⁸O adsorption on the heating leads.

The incorporation of lattice ¹⁸O into the water TPD product from formic acid decomposition is shown in Figure 10. A substantial amount of incorporation occurred as shown by the H₂¹⁸O signal ($m/e = 20$). This signal extends from the onset of the TPD ramp at 195 K to about 450 K. Note also that some ¹⁸O was incorporated into the small water TPD peak at 620 K. The desorption of H₂¹⁸O from the onset of the temperature ramp implies that water molecules were formed at 195 K using lattice oxygen. This could be explained partially by proton transfer between a coadsorbed H₂¹⁶O molecule (see below) and an ¹⁸O-labeled hydroxyl according to eq 4. Uptake measurements from



the TPD data of Figures 3–6 indicate that the water TPD peak area continued to increase as a function of increased formic acid exposure even after the yields of carbon-containing TPD products saturated. This presumably resulted from a water impurity in the HCOOH source (see Experimental Section). For this reason, section 3.3 will examine the effect of coadsorbed water on the decomposition of formic acid. Note that if the exchange process shown in eq 4 occurs, then a greater amount of H₂¹⁶O should desorb at higher temperature from recombination of ¹⁶OH groups left on the surface. The H₂¹⁶O TPD trace of Figure 10 indicates that relatively more [¹⁶O]water desorbed between 300 and 450 K than did [¹⁸O]water.

Successive TPD experiments were performed on the same surface (following the experiment shown in Figures 8–10) without replenishing the surface with ¹⁸O. These TPD experiments showed a gradual decrease in the intensities of all ¹⁸O-containing TPD signals and corresponding increases in the ¹⁶O-containing signals indicative of ¹⁸O depletion from the surface.

Static secondary ion mass spectrometry (SSIMS) was used to determine the temperature range in which incorporation of lattice oxygen into the adsorbed layer occurred. The dominant +SSIMS ion signal from adsorbed formate was HCO⁺. Figure 11 shows the +SSIMS results from the HC¹⁶O⁺ and HC¹⁸O⁺ ions during temperature-programmed heating of a 1.1×10^{15} molecules/cm² formic acid exposure on the ¹⁸O-enriched TiO₂(100) (1 × 3) surface. It should be noted that these +SSIMS ion signals resulted from different processes than the HCO⁺ TPD signals followed in Figure 8 (and Figure 16 below). The SSIMS ion signals result from the sputtering event, and not from electron impact ionization of a neutral gaseous molecule, as occurs in the QMS during TPD. (The QMS filament is off during SSIMS measurements.)

During programmed heating of a formic acid exposure of 1.1×10^{15} molecules/cm², the HC¹⁶O⁺ ion signal decreased slightly between 170 and 300 K and then increased between 300 and 500 K, before falling to zero counts at 650 K. The decrease in the signal between 170 and 300 K resulted from formic acid desorption and decomposition, and the decrease

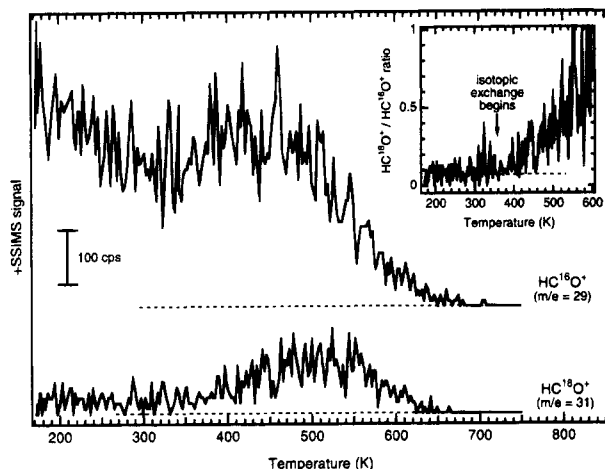


Figure 11. Isotopic exchange during decomposition of a 1.1×10^{15} molecules/cm² exposure of [¹⁶O]formic acid adsorbed on the ¹⁸O-enriched TiO₂(100) (1 × 3) surface as monitored by the HC¹⁶O⁺ ($m/e = 29$) and HC¹⁸O⁺ ($m/e = 31$) +SSIMS ion signals. The HC¹⁶O⁺ ion signal is displaced vertically for clarity, and zero-signal levels for each ion signal are marked with horizontal dashed lines. The primary Ar⁺ energy and flux were 500 eV and 1.2 nA/cm², respectively. The inset shows the ratio of the HC¹⁸O⁺ to HC¹⁶O⁺ ion signals as a function of temperature.

between 500 and 650 K was due primarily to formate decomposition. The HC¹⁸O⁺ ion signal was below 50 cps from 170 to 350 K but increased gradually above 350 K to a maximum signal at 500–550 K. The HC¹⁸O⁺ ion signal then dropped to zero in the same manner as did the HC¹⁶O⁺ ion signal. The low HC¹⁸O⁺ ion signal level between 170 and 350 K is important for two reasons. First, it indicates that the sputtering process did not “mix” the lattice oxygen atoms with the carbon-containing fragments in a matrix effect or an ion-induced surface heating effect. Second, the low HC¹⁸O⁺ ion signal level between 170 and 350 K indicates that exchange between lattice oxygen and adsorbed formate did not occur until the formate decomposition process began, as mentioned in the discussion of Figure 8. The onset temperature for oxygen exchange is more clearly seen in the inset to Figure 11, which shows the HC¹⁸O⁺ to HC¹⁶O⁺ ion ratio versus temperature. The rise in the ratio at about 360–400 K coincides with the onset of CO and H₂CO desorption (Figures 3 and 6). Also, the ratio maximized at about 550 K, as did the CO and H₂CO TPD signals. These data, along with the TPD data of Figures 8–10, indicate that exchange between lattice oxygen and formate does not occur until the formate decomposition process begins. This again implies that lattice oxygen is involved in the formate decomposition process.

The incorporation of lattice ¹⁸O during formate decomposition was also followed by –SSIMS, as shown in Figure 12. The HCOO[–] ion was the dominant –SSIMS ion from formic acid adsorbed on TiO₂(100). By monitoring the HCOO[–] ions, the extent of incorporation (one versus two ¹⁸O atoms) could be followed. Figure 12 shows the H₂¹⁶O¹⁶O[–], HC¹⁶O¹⁸O[–], and HC¹⁸O¹⁸O[–] ion signals during temperature-programmed heating of a 1.1×10^{15} molecules/cm² formic acid exposure on the ¹⁸O-enriched TiO₂(100) (1 × 3) surface. The HC¹⁶O¹⁶O[–] ion signal was intense between 165 and 300 K, while the ¹⁸O-containing signals were zero or near zero. The HC¹⁶O¹⁶O[–] ion signal decreased gradually above 300 K in a manner slightly different from that observed for the HCO⁺ ion signal in Figure 11. The gradual drop-off prior to and during formate decomposition was largely caused by a positive work function change between 300 and 750 K (Figure 13) that resulted from water desorption, as was observed for water on TiO₂(110),²⁵ and from formate

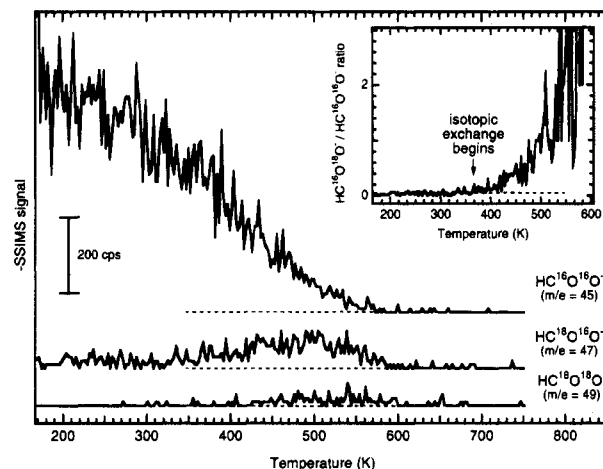


Figure 12. Isotopic exchange during decomposition of a 1.1×10^{15} molecules/cm² exposure of [¹⁶O]formic acid adsorbed on the ¹⁸O-enriched TiO₂(100) (1 × 3) surface as monitored by the HC¹⁶O¹⁶O[–] ($m/e = 45$), HC¹⁶O¹⁸O[–] ($m/e = 47$), and HC¹⁸O¹⁸O[–] ($m/e = 49$) –SSIMS ion signals. The HC¹⁶O¹⁶O[–] and HC¹⁶O¹⁸O[–] ion signals are displaced vertically for clarity, and zero-signal levels for each ion signal are marked with horizontal dashed lines. The primary Ar⁺ energy and flux were 500 eV and 0.6 nA/cm², respectively. The inset shows the ratio of the HC¹⁶O¹⁸O[–] to HC¹⁶O¹⁶O[–] ion signals as a function of temperature.

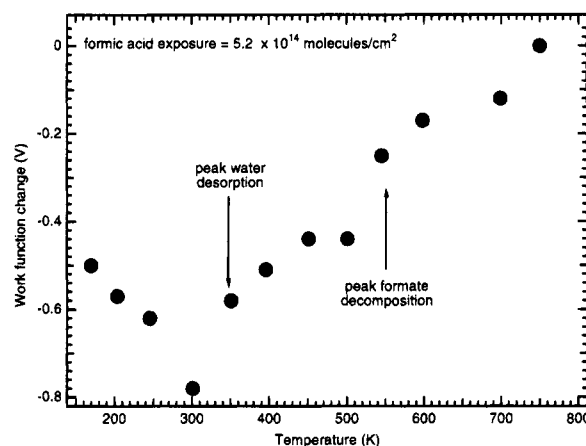


Figure 13. Work function changes as a function of heating temperature for a 5.2×10^{14} molecules/cm² exposure of formic acid on the TiO₂(100) (1 × 3) surface at 170 K. Work function changes were determined by measuring the onset of secondary electron emission during exposure of the surface to a 100 eV electron beam. A –10 V sample bias was used to sharpen the onset edge.

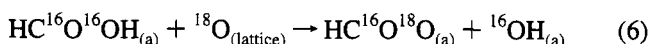
decomposition.³ A positive work function change presumably increases the neutralization probabilities for negative ions leaving the surface, which in turn results in decreased ion signals. Despite the positive work function change, the incorporation of lattice ¹⁸O during formate decomposition is evident in the HC¹⁶O¹⁸O[–] and HC¹⁸O¹⁸O[–] ion signals which increased from zero signal at about 350 K. Increased ion signal corresponding to HC¹⁸O¹⁸O[–] indicates that some formate species underwent multiple exchange processes with the surface. However, the HC¹⁸O¹⁸O[–] ion signal lagged slightly behind the HC¹⁶O¹⁸O[–] ion signal in temperature, suggesting that one exchange process was favored. The inset of Figure 12 shows the HC¹⁶O¹⁸O[–] to HC¹⁶O¹⁶O[–] ion signal ratio as a function of heating. As was seen for the positive ions (Figure 11), the exchange process began at about 360–400 K and reached a maximum at about 550 K.

The SSIMS data in Figures 11 and 12 assist in understanding the process of formic acid decomposition to formate and the presence of water desorption prior to formate decomposition

in TPD. The products of formic acid decomposition is formate and a surface proton. The proton presumably forms a hydroxyl group with lattice oxygen according to eq 5. For



example, formic acid decomposition on MgO(100) occurs by cleavage of the O–H bond to form C_{2v} bidentate formate, as determined by HREELS.⁸ On MgO(100), the deposited protons do not react with lattice oxygen in a concerted manner to make water but remain on the surface until formate decomposes at about 600 K. At this point CO and H₂O are liberated in a stoichiometric process. However, based on the occurrence of water desorption from the TiO₂(100) (1 × 3) surface prior to formate decomposition, the acid proton deposited on the surface must be involved in making water without the use of the formate oxygen or hydrogen atoms. If formic acid decomposes on TiO₂ surfaces by a process similar to that on MgO(100) (strict O–H bond cleavage), then water must be made from the reaction of the deposited protons with lattice oxygen atoms. This was proposed by Kim and Barteau⁵ for water desorption prior to formate decomposition on TiO₂(001). A second possibility is that some formic acid molecules decompose by C–OH bond cleavage, depositing a hydroxyl group on the surface and forming formate with a lattice oxygen atom, as shown in eq 6



with lattice ¹⁸O. The hydroxyl groups could then react with each other to make water. Cleavage of the CO–H bond fits with the incorporation of lattice ¹⁸O into water (Figure 10). Cleavage of the C–OH bond might explain the presence of ¹⁸O in the CO and H₂CO TPD products if formate were formed with lattice oxygen, but it does not explain the absence of isotopic oxygen exchange in the SSIMS data until the onset of formate decomposition (Figures 11 and 12). Cleavage of the CO–H bond has strong implications for chemical processes which generate surface protons since these protons appear to abstract lattice oxygen atoms from TiO₂ surfaces to form water with relative chemical ease. Removing surface oxygen atoms in turn creates point defects (low coordination, reduced cation centers) which are available for reductive chemistry. It is interesting to note that if these vacancies were formed on the (1 × 1) surface by a similar mechanism, formate did not react with the reduced Ti atoms at these sites to produce formaldehyde (Figure 7). This may imply that formate does not readily diffuse on TiO₂ and that these sites are only filled after formate decomposition, presumably with the formate oxygen atom left on the surface (eq 2).

The mechanism by which lattice oxygen is incorporated into the high-temperature formic acid TPD products (CO and H₂CO) is not apparent from the data in this paper. It is clear that incorporation does not occur upon adsorption or prior to the onset of formate decomposition; therefore, models involving formic acid adsorption and decomposition are probably not valid. It is possible that formate decomposition proceeds through a transition state involving nucleophilic attack by two-coordinate bridging O²⁻ atoms on the formate carbon atom. It is also possible that a metastable intermediate, such as a formyl species (HCO), could react with a bridging O²⁻ atom to regenerate formate on a time scale comparable to that for its decomposition to CO.

3.3. Influence of Coadsorbed Water on Formic Acid Chemistry. As mentioned above, the TPD data of formic acid (Figure 4) suggest that a small amount of water, originating from the formic acid source, was coadsorbed with formic acid

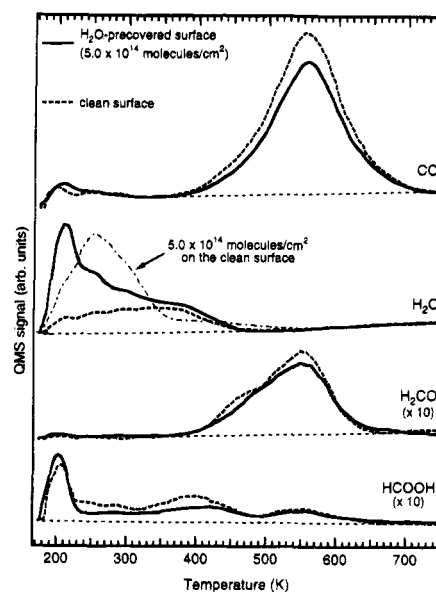


Figure 14. Effect of preadsorbed water (5.0×10^{14} molecules/cm²) on the TPD products from a 7.0×10^{14} molecules/cm² exposure of formic acid to the TiO₂(100) (1 × 3) surface. TPD spectra from the same formic acid exposure on the clean surface and from a 5.0×10^{14} molecules/cm² water exposure on the clean surface are shown for comparison. Spectra were displaced vertically for clarity.

on the TiO₂(100) (1 × 3) surface. Studies were undertaken to determine the extent to which this coadsorbed water influenced the chemistry of formic acid on the TiO₂(100) (1 × 3) surface. The influence of water is potentially important in photocatalysis and electrochemistry at the aqueous–solid interface.^{26–30}

Figure 14 shows TPD results from the decomposition of formic acid on the water-precovered TiO₂(100) (1 × 3) surface. Data from formic acid decomposition on the clean surface are shown for comparison (dashed lines). The surface was exposed to 5.0×10^{14} molecules/cm² of water at 180 K prior to a 7.0×10^{14} molecules/cm² exposure of formic acid. TPD from this same exposure of water on the clean surface (dot-dash line) indicates that water desorbed in a broad peak centered at about 250 K, with a high-temperature tail extending past 450 K. The high-temperature tail was previously interpreted as a pumping speed effect²² but may reflect water desorption (molecular or dissociative) from strongly bound states at minority sites, such as structural or point defects. The TPD peak intensities for CO, HCOOH, and H₂CO from formic acid decomposition on the water-precovered TiO₂(100) (1 × 3) surface all decreased slightly compared to the clean surface traces. This suggests that water acts as a weak site blocker of formic acid adsorption and/or decomposition sites. Both blocking effects probably occurred since a significant portion of the molecular formic acid desorption between 220 and 350 K was shifted below 220 K and since the amount of each decomposition product decreased. Site blocking could occur by (a) blocking Ti cation sites, which are presumably the preferred adsorption and decomposition sites of formic acid, or (b) blocking proton receptor sites (presumably two-coordinate bridging oxygen atoms), which inhibits cleavage of the O–H bond of formic acid. Previous work suggests that low coverages of water dissociatively adsorb on the (1 × 3) surface.^{16,17} Dissociative water adsorption would block both cation sites (with a hydroxyl group) and anion sites (with a proton).

It is interesting to note that the equilibrium between formate and formic acid was not shifted toward formic acid by the presence of water. That is, less formic acid desorbed in the 400 K TPD peak attributed to dissociative recombination of

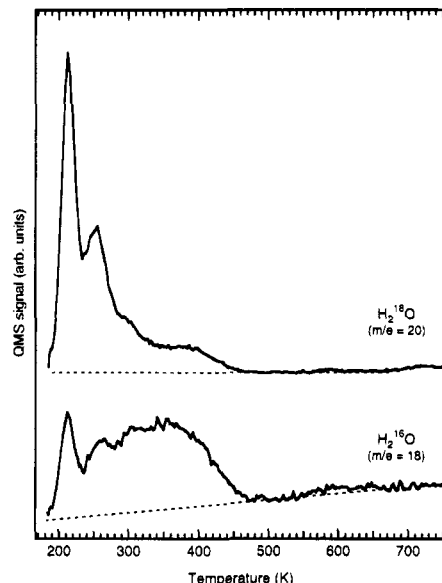
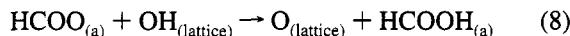
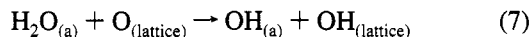


Figure 15. TPD spectra for H_2^{16}O ($m/e = 18$) and H_2^{18}O ($m/e = 20$) from a 6.5×10^{14} molecules/cm² exposure of formic acid on the TiO_2 -(100) (1×3) surface preadsorbed with H_2^{18}O (5.9×10^{14} molecules/cm²). The H_2^{18}O spectrum was displaced vertically for clarity.

formate and a proton. Although formic acid is a considerably stronger Bønsted acid than water, the equilibrium between formate and formic acid could presumably be shifted toward formic acid during water exposure, as shown in eqs 7 and 8



or by a direct process, as shown in eq 9.



Both processes would become irreversible by removing formic acid from the surface into vacuum (eq 10).



However, exposing various coverages of formate on the TiO_2 -(100) (1×3) surface at 250–450 K to water exposures equivalent to many monolayers did not deplete the surface of formate to any extent greater than that which occurred during annealing at the same temperature in the absence of water (data not shown). This suggests that the processes in eqs 7–9 are not favorable on the TiO_2 (100) (1×3) surface between 250 and 450 K under UHV conditions. It also indirectly suggests that water dissociation on the TiO_2 (100) (1×3) surface (eq 7) is not extensive (at least not when formate is present) since eq 8 readily occurs, as indicated by the 390 K TPD state of formic acid (Figure 5).

The extent to which water is chemically involved in formic acid decomposition is not apparent from the site-blocking data of Figure 14. Isotopically labeled water (H_2^{18}O) was used to determine whether preadsorbed water was chemically involved in formic acid decomposition. Figure 15 shows water TPD (H_2^{16}O and H_2^{18}O) resulting from decomposition of a 6.5×10^{14} molecules/cm² formic acid exposure on the H_2^{18}O -precovered TiO_2 (100) (1×3) surface. The majority of the preadsorbed H_2^{18}O was displaced to the second layer (and presumably into the vacuum since the adsorption temperature was 180 K) during formic acid adsorption. However, some H_2^{18}O molecules remained strongly bound to the surface, presumably as hydroxyl groups, as evidenced by the H_2^{18}O

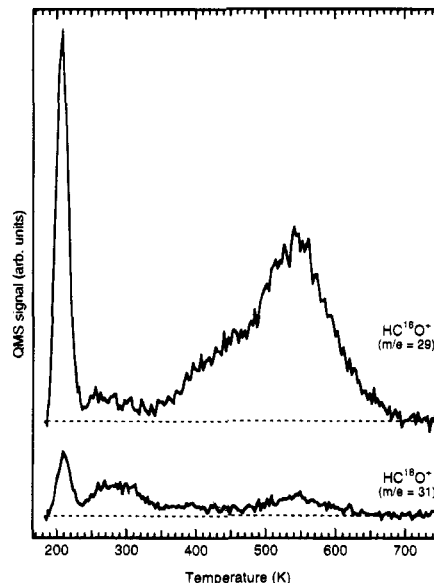


Figure 16. TPD spectra for the HC^{16}O^+ ($m/e = 29$) and HC^{18}O^+ ($m/e = 31$) QMS cracking fragments from a 6.5×10^{14} molecules/cm² formic acid exposure on the TiO_2 (100) (1×3) surface preadsorbed with H_2^{18}O (5.9×10^{14} molecules/cm²). The HC^{16}O^+ spectrum was displaced vertically for clarity.

signal above 300 K. However, most of the water which desorbed above 250 K contained ^{16}O . A trace amount of H_2^{18}O was observed in the 620 K water TPD state.

Figure 16 shows the TPD traces for the HC^{16}O^+ and HC^{18}O^+ QMS cracking fragments from the same experiment as that of Figure 15. A small amount of HC^{18}O^+ signal was observed at 550 K indicative of ^{18}O incorporation into the high-temperature formic acid and formaldehyde TPD states. (Trace amounts of $\text{HC}^{16}\text{O}^{18}\text{OH}$ and $\text{H}_2\text{C}^{18}\text{O}$ were also detected.) However, the vast majority of these products evolved in TPD without ^{18}O incorporation from coadsorbed H_2^{18}O . Also, extensive oxygen exchange did not take place in the formic acid desorption at 205 K. However, comparison of the HC^{16}O^+ and HC^{18}O^+ traces in the temperature range between 240 and 350 K indicates that a proportionally greater amount of ^{18}O -containing signal was present. This HCO^+ signal, which resulted from molecular HCOOH desorption, suggests that weakly bound water and formic acid molecules readily exchange OH groups. This exchange, prior to desorption and/or decomposition of all molecularly bound formic acid, was probably responsible for the small HC^{18}O^+ signal observed at 550 K.

These results suggest that water is weak site blocker of formic acid and that water has little or no influence on the chemistry of formic acid or formate on the TiO_2 (100) (1×3) surface under UHV conditions. However, one might expect more significant effects at the much higher water fluxes encountered under aqueous conditions.

4. Conclusions

1. Lattice oxygen atoms are involved in the formate decomposition process on the TiO_2 (100) (1×3) surface due to coincident onset temperatures for isotopic exchange between formate and lattice ^{18}O and the evolution of gas phase products containing ^{18}O . One possible role of lattice oxygen in formate decomposition could be the weakening of C–O bonds due to nucleophilic attack by two-coordinate bridging O^{2-} atoms on the formate carbon atom.

2. Protons deposited on the TiO_2 (100) (1×3) surface from formic acid decomposition show facile ability to produce water from reaction with lattice oxygen atoms.

3. Preadsorbed water is a weak site blocker of formic acid adsorption and/or decomposition sites and does not appear to influence formic acid chemistry on the TiO₂(100) (1 × 3) surface.

Acknowledgment. The author gratefully acknowledges helpful conversations with M. A. Barteau and D. F. Cox. This work was supported by the U.S. Department of Energy, Office of Basic Energy Sciences, Division of Materials Science.

References and Notes

- (1) Onishi, H.; Aruga, T.; Egawa, C.; Iwasawa, Y. *Surf. Sci.* **1988**, *193*, 33.
- (2) Onishi, H.; Aruga, T.; Iwasawa, Y. *J. Am. Chem. Soc.* **1993**, *115*, 10460.
- (3) Onishi, H.; Aruga, T.; Iwasawa, Y. *J. Catal.* **1994**, *146*, 557.
- (4) Onishi, H.; Iwasawa, Y. *Chem. Phys. Lett.* **1994**, *226*, 111.
- (5) Kim, K. S.; Barteau, M. A. *Langmuir* **1988**, *4*, 945.
- (6) Kim, K. S.; Barteau, M. A. *Langmuir* **1990**, *6*, 1485.
- (7) Kim, D. H.; Anderson, M. A. *Environ. Sci. Technol.* **1994**, *28*, 479–83.
- (8) Petrie, W. T.; Vohs, J. M. *Surf. Sci.* **1991**, *259*, L750.
- (9) Truong, C. M.; Wu, M.-C.; Goodman, D. W. *J. Chem. Phys.* **1992**, *97*, 9447.
- (10) Dilara, P. A.; Vohs, J. M. *J. Phys. Chem.* **1993**, *97*, 12919.
- (11) Domen, K.; Akamatsu, N.; Yamamoto, H.; Wada, A.; Hirose, C. *Surf. Sci.* **1993**, *283*, 468.
- (12) Gercher, V. A.; Cox, D. F. *Surf. Sci.* **1994**, *312*, 106.
- (13) Ludviksson, A.; Zhang, R.; Campbell, C. T.; Griffiths, K. *Surf. Sci.* **1994**, *313*, 64.
- (14) Chung, Y. W.; Lo, W. J.; Somorjai, G. A. *Surf. Sci.* **1977**, *64*, 588.
- (15) Lo, W. J.; Chung, Y. W.; Somorjai, G. A. *Surf. Sci.* **1978**, *71*, 199.
- (16) Muryn, C. A.; Tirvengadam, G.; Crouch, J. J.; Warburton, D. R.; Raiker, G. N.; Thornton, G.; Law, D. S.-L. *J. Phys.: Condens. Matter* **1989**, *1*, SB127.
- (17) Muryn, C. A.; Hardman, P. J.; Crouch, J. J.; Raiker, G. N.; Raiker, G. N.; Thornton, G.; Law, D. S.-L. *Surf. Sci.* **1991**, *251/252*, 747.
- (18) Zschack, P. *Springer Ser. Surf. Sci.* **1991**, *24* (The Structure of Surfaces III), 646.
- (19) Murray, P. W.; Leibsle, F. M.; Fisher, H. J.; Flipse, C. F. J.; Muryn, C. A.; Thornton, G. *Phys. Rev. B* **1992**, *46*, 12877.
- (20) Zschack, P.; Cohen, J. B.; Chung, Y. W. *Surf. Sci.* **1992**, *262*, 395.
- (21) Hardman, P. J.; Prakash, N. S.; Muryn, C. A.; Raiker, G. N.; Thomas, A. G.; Prime, A. F.; Thornton, G.; Blake, R. J. *Phys. Rev. B* **1993**, *47*, 16056.
- (22) Henderson, M. A. *Surf. Sci.* **1994**, *319*, 315.
- (23) Murray, P. W.; Leibsle, F. M.; Muryn, C. A.; Fisher, H. J.; Flipse, C. F. J.; Thornton, G. *Surf. Sci.* **1994**, *321*, 217.
- (24) Idriss, H.; Barteau, M. A. **1995**, *Surf. Sci.*, submitted.
- (25) Hugenschmidt, M. B.; Gamble, L.; Campbell, C. T. *Surf. Sci.* **1994**, *302*, 329.
- (26) Miles, M. H.; Fletcher, A. N.; McManis, G. E.; Spreer, L. O. *J. Electroanal. Chem. Interfacial Electrochem.* **1985**, *190*, 157–70.
- (27) Matthews, R. W. *J. Catal.* **1986**, *100*, 275–8.
- (28) Chester, G.; Anderson, M. A.; Read, H.; Esplugas, S. *J. Photochem. Photobiol., A* **1993**, *71*, 291–7.
- (29) Aguado, M. A.; Anderson, M. A.; Hill, G. C., Jr. *J. Mol. Catal.* **1994**, *89*, 165–78.
- (30) Bogdanoff, P.; Alonso-Vante, N. *J. Electroanal. Chem.* **1994**, *379*, 415.

JP951533A